



PREPARATION, STRUCTURAL AND ELECTRICAL PROPERTIES OF $Zn_{1-x}Li_xO$ SOLID SOLUTION

*M. K. R. KHAN, M. M. RAHMAN and I. TANAKA¹

Department of Physics, University of Rajshahi, Rajshahi-6205, Bangladesh

¹Center for Crystal Science and Technology, University of Yamanashi, Miyamae 7, Kofu Yamanashi 400-8511, Japan

(Received December 26, 2002 and accepted in revised form April 4, 2003)

$Zn_{1-x}Li_xO$ samples have been synthesized by conventional solid state reaction method and studied their structure, grain size, and electrical properties. The crystalline grain size and lattice constants were determined from the profile of x-ray diffraction. X-ray study shows that Li is soluble in ZnO upto 30 mol.%. The approximate grain size of the crystal in the direction perpendicular to (100), (002), (101), (102) and (110) planes ranges from 45 to 56 nm. The lattice parameters of these materials are consistent with the reported values. The dc electrical conductivity measurement shows that all samples are highly resistive ($\sim 10^6$ ohm-cm) upto a certain critical temperature (T_c) above which conductivity of the materials increases gradually. The band gap energy (3.19-3.5 eV) calculated from conductivity measurement is comparable to the optical band gap of ZnO crystal, which reveals that after T_c , electron transition occurs from valence band to conduction band only.

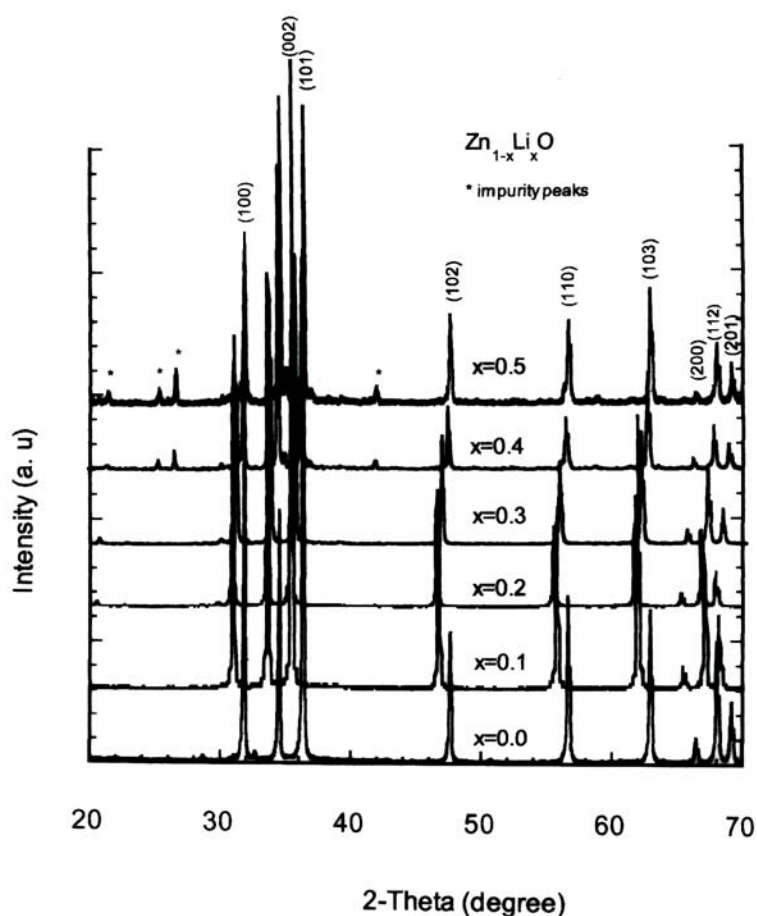
Keywords: Zinc oxide, Solid solution, Grain size, Energy gap, DC conductivity.

1. Introduction

Zinc oxide is one of the most promising materials among II-VI wide-band semiconductors. It has attracted attention not only as a suitable lattice-matched substrate for GaN but also as a potentially useful active optoelectronic material in its own right [1]. These unique properties raise new questions not only about the basic properties of ZnO but also about those of related materials which can be combined with ZnO in heteroepitaxial device structures. But the application of zinc oxide as a semiconductor is limited by the difficulties in obtaining samples with the proper electrical and optical properties [2]. Energy absorption in this wide band gap semiconductor occurs by exciting electrons to the empty conduction band leaving holes in the completely filled valence band. Recombination usually occurs either close to the crystal lattice or in electronic defects of the crystal lattice [3]. Physical properties, such as electrical conductivity, piezoelectricity and defect structure of these materials changed by the amount of excess Zn and also by the dopant elements in lattice structure. Such type of defects normally influences the crystal morphology, structure,

grain-size, composition etc. In general, morphology, crystal structure, crystallite size and crystallinity depend on precursor and experimental parameters used during solid state reaction [4]. There are many techniques widely used for the investigation of these characteristics such as, x-ray diffractometry, scanning and transmission electron microscopies and specific surface area measurements. Among these techniques, x-ray diffractometry is very simple, cost effective and non-destructive. Performing line-broadening analysis of x-ray diffraction, one can easily estimate the crystallite shape and size of a sample. Zinc oxide (ZnO) doped with small percentage of Li presents rich x-ray diffractogram with various orders of reflections, which allow crystallite shape and size analysis. The grain size analysis of zinc oxide powder as a function of morphological evolution has been done by Fernando et al. [5]. The detailed study of grain size depending on doping is still unexplored. In the present work, we have determined solubility of Li into ZnO and estimated crystallite size of Li doped ZnO prepared by solid state reaction method and studied their structural and electrical properties.

* Corresponding author : ykrkhan@yahoo.com:

Figure 1. X-ray diffraction patterns of $Zn_{1-x}Li_xO$

2. Experimental

A series of Zn-Li-O samples were synthesized by solid-state reaction method. Stoichiometric amounts of high purity reagent grade ZnO , Li_2CO_3 were mixed to prepare $Zn_{1-x}Li_xO$ samples. Mixed powders were thoroughly ground and calcinated twice at around $850\text{ }^\circ\text{C}$ in air for 12 hours with intermittent grinding. The obtained white powders were then pressed into circular pellets with the dimension of about 12 mm in diameter and 2-3 mm in thickness with a pressure of about 2500 pound / sq. inch. The prepared pellets were then sintered in air atmosphere at $875\text{-}900\text{ }^\circ\text{C}$ for 12 hours and furnace cooled to obtain crystalline phase.

The crystalline phase of the materials were checked by X-ray diffractometer (RIGAKU, Geigerflex) using CuK_α radiation ($\lambda=1.5405\text{ \AA}$, or 0.154 nm) at room temperature. The diffraction scan was recorded in the angular range $20^\circ \leq 2\theta \leq 70^\circ$ with a scanning speed of $2^\circ/\text{min}$.

and step sampling of 0.02° . The lattice parameters were determined from the XRD patterns using Hess-Lipson method. The crystal or grain size was determined quantitatively using Scherrer method [6]. Digital multimeter (Keithley 614 Electrometer) was used for the measurement of conductivity of the samples. The dielectric properties were studied by a multi-frequency LCR meter (SR 720) at room temperature. The relative dielectric constant ϵ_r was calculated from the measured capacitance of the samples.

3. Results and Discussion

The X-ray diffraction patterns of the Li doped ZnO samples are shown in Fig. 1. It is evident from the XRD patterns that the samples are of single phase for $x = 0.0$ to $x = 0.3$. A small amount of other phases like Lithium Zinc Oxide is found for $x \geq 0.3$, which is realized by the presence of few extra peaks in the XRD pattern lying in

Table 1. Lattice constants, c/a ratio, Zn-O bond length, and E_g of $Zn_{1-x}Li_xO$ samples

Sample	Molar ratio, x	Lattice constant (Å)		c/a ratio	Zn-O bond length (Å)	Band gap E_g (eV)
		a	c			
$Zn_{1-x}Li_xO$	0.0	3.2458	5.2022	1.6027	1.9755	3.20 [11]
	0.10	3.2412	5.2119	1.6080	1.9780	3.50
	0.20	3.2503	5.2076	1.6021	1.9781	3.19
	0.30	3.2504	5.2079	1.6022	1.9871	3.46
	0.40	3.2498	5.2075	1.6024	1.9781	3.22
	0.50	3.2497	5.2072	1.6023	1.9780	3.46

*Zn-O bond length 1.9778 Å [6]

between 20° to 30° and around 45° of 2θ scan. It is also found that reflection lines for Li doped samples ($x \geq 0.3$) slightly shifted to the left from reflection lines of $x = 0$ sample. But for samples of $x = 0.4$ and 0.5 , reflection lines tend to align with the lines of $x = 0$. From these observations it is assumed that Li is soluble in ZnO up to $x \leq 0.30$. Theoretically, this solubility limit seems to be high. The structure of Zn is hcp while Li possesses both bcc and hcp structure [7]. Though the electronic valence is different between Li^{+1} and Zn^{2+} but for their same structure and proximity of ionic radii, the solubility upto 30 mol% is not unexpected. The x-ray diffraction profiles could be indexed with hexagonal unit cell. The prominent peaks in the diffractogram (Fig. 1) correspond to the (100), (002), (101), (102) and (110) reflecting planes of hexagonal structure. The lattice parameters, Zn-O bond length and c/a ratio is shown in Table 1. The determined lattice parameters are slightly different from that of the pure ZnO [8]. The ionic radius of Zn is 0.74 Å while the ionic radius of Li is 0.60 [8] and 0.68 [9]. The small change of lattice parameters compared to pure ZnO indicates that the dopant Li substitutes the Zn atoms since the ionic radius of Zn (0.74 Å) is comparable to the ionic radii of Li (0.68 Å). The high solubility limit ($x \leq 0.3$) of Li into ZnO seems reasonable when ionic radius of Li is considered as 0.68 Å. In this case, the difference between ionic radii is less than 10%. In this context, slight changes in Zn-O bond length (of the order of 10^{-3} Å) as well as in c/a ratio is

justified. These small changes in lattice parameters and Zn-O bond length are induced by the distortion of structure due to the substitution of Zn atoms by off-centered Li atoms in ZnO structure. This could also be realized by the small shift of reflection planes in the X-ray diffractogram (Fig. 1). It is reported that such a small structural distortion is connected to the ferroelectric phase transition [8].

The X-ray diffraction patterns clearly indicate that the samples are of crystalline type; the reflection line profiles were subjected to calculate crystal or grain size perpendicular to the different crystalline planes. The grain size, ξ , of the samples were determined quantitatively using the formula [6],

$$\xi = \frac{K\lambda}{B \cos \theta} \quad (1)$$

where, λ is the wavelength of the incident x-ray beam, K is a constant equal to unity and θ is usual Bragg angle. The unit for ξ is same as that of the λ and expressed in nano-meters. The breadth B of a diffraction line may be measured by means of an ionization chamber or by densitometry of a pattern recorded photographically. In general, B is obtained by measuring so-called full width at half-maximum (FWHM) expressed in radians. Since the broadening of a peak is sensitive to the variation near the tails at the bottom of the peak hence it

Table. 2. Crystallite or grain size ξ of $Zn_{1-x}Li_xO$ crystals.

Sample (hkl)	ZnO	Zn _{0.9} Li _{0.1}	Zn _{0.8} Li _{0.2}	Zn _{0.7} Li _{0.3}	Zn _{0.6} Li _{0.4}	Zn _{0.5} Li _{0.5}
	ξ (nm)	ξ (nm)	ξ (nm)	ξ (nm)	ξ (nm)	ξ (nm)
100	52	48	51	54	51	50
002	54	52	54	56	52	51
101	45	46	52	52	50	53
102	50	48	53	53	48	56
110	50	45	49	50	51	54

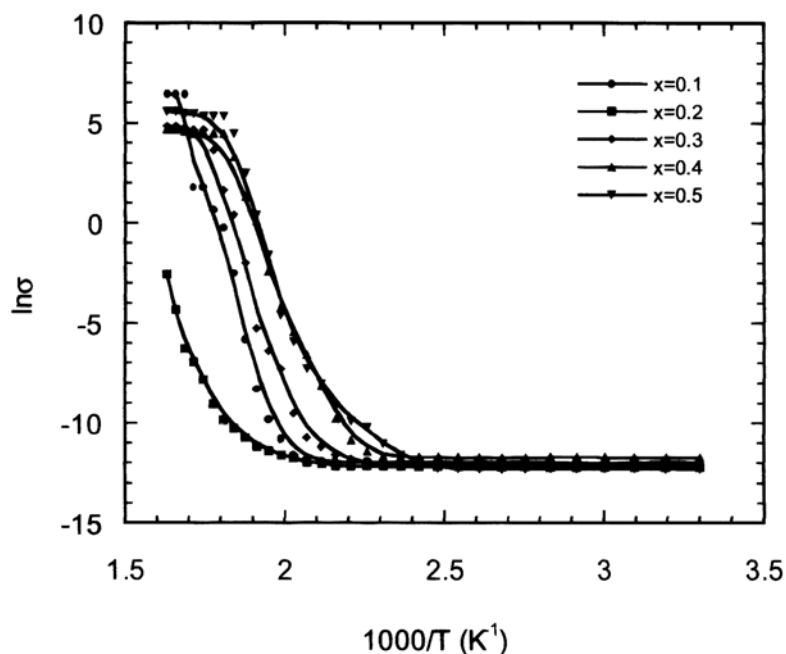


Figure 2. Variation of $\ln\sigma$ with $1/T$ for $Zn_{1-x}Li_xO$

was corrected for background. The instrumental broadening was corrected for the standard ZnO sample. The values of crystallite size calculated perpendicular to different crystal planes is tabulated in Table 2. From Table 2, it is clear that the apparent crystallite size is similar irrespective of crystalline planes. It is also seen that crystallite size is almost independent of doping concentrations. Since all the samples were prepared in identical conditions and cooled in furnace down to room temperature, the above result is quite reasonable. The intensity of the (002) peak was lower than (100) peak for $x = 0.0$ and substantially increased as a function of doping and it becomes dominant for $x > 0.3$.

However, the crystallite size is more or less independent of doping concentrations. Therefore, the increase of reflection intensity for (002) plane compared to (100) plane may be related to the preferred orientation in the samples. The crystallite size in the direction perpendicular to the (002) plane is slightly larger than for (100) plane (Table 2), and as a result the crystallite shape regarded as cylindrical. Similar result is reported for ZnO prepared by thermal decomposition method [5].

Figure 2 shows the logarithmic variation of conductivity with inverse of absolute temperature. It is seen from the figure that the conductivity is very low of the order of 10^{-6} - $10^{-7} \Omega^{-1} \text{cm}^{-1}$ and

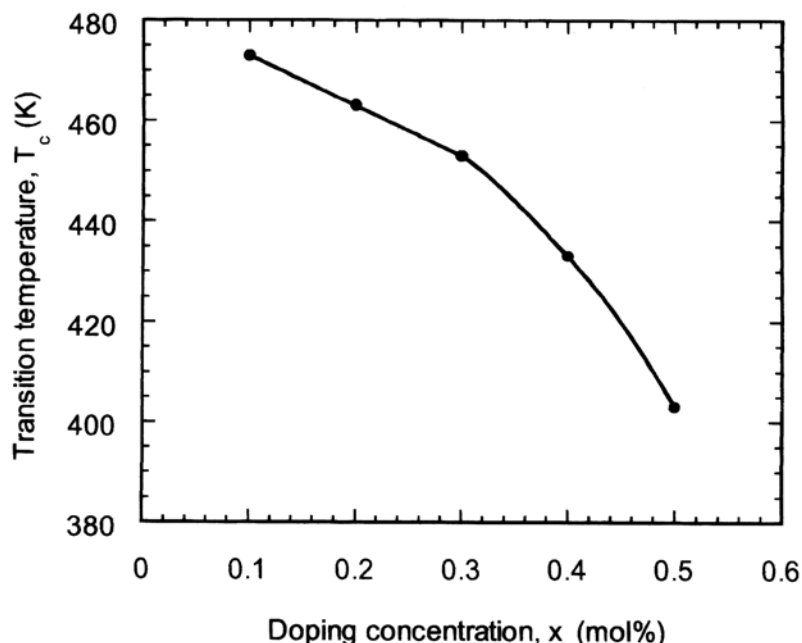


Figure 3. Change of T_c with Li concentration, x .

almost constant upto a critical temperature T_c after which it increases gradually. At the tail end i.e., in the high temperature region of the conductivity curve, within the measured temperature range, a tendency of resistance saturation is observed for all samples (Fig. 2). At room temperature pure ZnO is an insulator. It is established that the conductivity of ZnO influenced by the presence of excess Zn atoms in formula unit and/ or introduction of impurity atoms. In the present case, it seems the conductivity of doped ZnO is mostly due to excess Zn rather than Li doping. However, the doping concentrations affect the transition temperature T_c significantly. After the transition temperature T_c , following relation can be used to express the mechanism of carrier transport [10],

$$\sigma = \sigma_0 \exp\left(-\frac{E_g}{k_B T}\right) \quad (2)$$

where, E_g is the energy gap and k_B is the Boltzmann constant. The energy gap E_g has been calculated from the slope of $\ln \sigma$ vs. $1/T$ plot. The obtained values of E_g are in the range of 3.19-3.5 eV and it is very close to the optical band gap (3.2 eV) of the ZnO crystal. This result reveals that the conduction after T_c is thermally assisted and occurs due to the transition of electrons from valence band to conduction band. The variation of

transition temperature T_c with doping concentration is shown in Fig. 3, which indicates that the critical temperature, T_c , gradually decreases with the increase of Li concentration in ZnO.

The dielectric constant of the samples was calculated from the measured capacitance at zero bias. Fig. 4 shows the variation of dielectric constant with frequency (100 Hz-100 kHz) for different doping concentrations. It is observed that the dielectric constant of $Zn_{1-x}Li_xO$ decreases in the low frequency region and in the high frequency region variation is insensitive. It is also found that the dielectric constant is maximum for $x = 0.2$, which indicates that the maximum lattice mismatch may occur in this concentration.

4. Conclusions

The X-ray diffraction patterns reveal that Li is soluble in ZnO upto $x \leq 0.3$, beyond this range additional Lithium Zinc Oxides phases are also formed. The structure of the samples could be indexed with hexagonal unit cell and the ratio c/a is 1.602.

The estimated grain size is of the nano-scale with cylindrical shape and independent of doping concentrations. After transition temperature T_c , thermally assisted direct transition of electron from valence band to conduction band is realized for Li

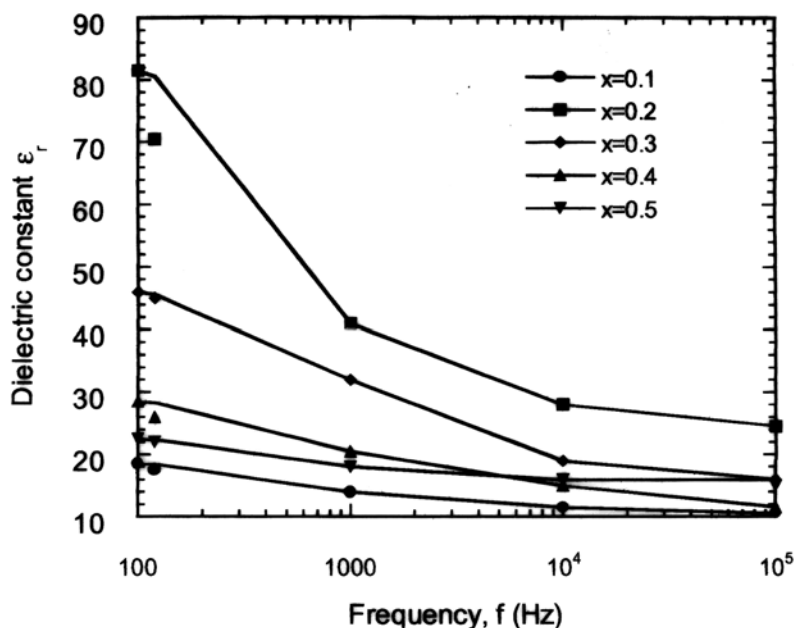


Figure 4. Frequency dependent dielectric constant of $Zn_{1-x}Li_xO$.

doped ZnO. The determined band gap energy is comparable to the optical band gap of the materials.

Acknowledgement

The authors M. K. R. Khan and M. M. Rahman would like to acknowledge University of Rajshahi, Bangladesh, for providing financial assistance to carry out this research work.

References

- [1] D. C. Reynolds, D. C. Look, B. Jogai, C. W. Litton, T. C. Collins, W. Harsch and G. Cantwell, *Phys. Rev., B* **57** (1998)12151. *Phys. Rev., B* **58** (1998)13276.
- [2] A.N. Georgobiani, T. V. Butkhuzi, E. Zadauly, N. P. Kekelidze and T. G. Khulordava, *Inorg. Mater. (Transl. of Neorg. Mater.)* **29** (1993) 1249.
- [3] G. Blasse and B. C. Grabmaier, *Luminescent Materials* (Springer, Berlin, 1994) p. 60.
- [4] D. Louer, J. P. Auffredic, J. I. Langford, D. Ciosmak, and J. C. Niepce, *J. Appl. Crystallogr.*, **26** (1983) 22.
- [5] A. S. Fernando, O. P. S. Carlos de, J. Jr. Miguel and R. D. Marian, *Powder Diffraction*, **16** (2001) 153.
- [6] B.D. Cullity, *Elements of X-ray diffraction*, Addison-Wesley Publishing Co. Inc. (1967) p. 262.
- [7] P. Haasen, *Physical Metallurgy*, 3rd ed., Cambridge University Press, UK (1997).
- [8] A. Onodera, N. Tamaki, K. Jin and H. Yamashita, *Jpn. J. Appl. Phys.*, **36** (1997) 6008.
- [9] C. Kittel, *Introduction to Solid State Physics*, 7th ed., John Wiley and Sons, Inc., (1996).
- [10] N. F. Mott and E. A. Davis, *Electronic Processes in Non-Crystalline Materials*, Clarendon Press, Oxford (1979).
- [11] S. J. Fonash, *Solar cell device Physics*, Academic Press Inc, London Ltd. (1981).